J Electroceram (2012) 29:95–98
DOI 10.1007/s10832-012-9752-1

Influence of Al_2O_3 additive on the dielectric behavior and energy density of $Ba_{0.5}Sr_{0.5}TiO_3$ ceramics

Di Yi · Jiancong Yuan · Haiyang Liu · Yang Shen · Yuan-Hua Lin · Ce-Wen Nan · Xiao Xi · Jinliang He

Received: 18 January 2012 / Accepted: 22 June 2012 / Published online: 10 July 2012

Abstract High dense $Ba_{0.5}Sr_{0.5}TiO_3$ ceramics with Al_2O_3 additives have been prepared by a method combined the sol–gel process and the solid state reaction. Phase compositions, microstructure and dielectric behaviors are investigated systematically. Our experiment results reveal that the Al_2O_3 additives reduce the dielectric constant slightly and increase the breakdown strength greatly due to the refined microstructure and the formation of the second phases. The estimated energy density of $Ba_{0.5}Sr_{0.5}TiO_3$ ceramics with optimized Al_2O_3 additives is improved by 1.5 times as compared with that of pure $Ba_{0.5}Sr_{0.5}TiO_3$ ceramics.

Keywords Dielectric behavior · Breakdown strength · $Ba_{0.5}Sr_{0.5}TiO_3$ · Energy density

1 Introduction

The perovskite structure materials have been extensively studied for dielectric, ferroelectric and multiferroic properties [1, 2]. Capacitive components with high dielectric constant, low loss tangent and good physical stabilities have been attractive for potential application in various fields such as the microelectronic devices and the energy-storage capacitors. Barium strontium titanate ($Ba_{1-x}Sr_xTiO_3$, abbreviated as BST) is one of the candidates which have been widely investigated to achieve the high dielectric constant and high breakdown voltage simultaneously. Previous studies [3, 4] have shown that the composition of $Ba_{1-x}Sr_xTiO_3$ has great effects on the energy storage behavior. The optimized value of x over the range of working field has been predicted by the theoretical calculation [4]. The energy density of BST is strongly limited by the low breakdown strength. Therefore, it is an important issue to increase the breakdown strength of BST ceramics before it can be used in the high energy density capacitors.

It is a common approach to use the glass additives, which can refine the microstructure of ceramics. A. Young et al. [5] found that the addition of glass dramatically increased the breakdown strength of ceramics. Q. Zhang et al. [6] studied the energy density of ceramics with glass additives and observed the improvement by the factor of 2.4. Glass-ceramic has also been studied by starting with the defect-free glass matrix [7]. E. Gorzkowski et al. [8] investigated the energy density of glass-ceramic and prepared samples with both high dielectric constant and high breakdown strength. Furthermore, H. Ogihara et al. [9] studied the solid solution of 0.7 $BaTiO_3$–0.3 $BiScO_3$ ceramics and observed a higher energy density than many commercial capacitors.

In this paper, we presented a new way to increase the breakdown strength and the energy density of BST. Normally, alumina (Al_2O_3) has much higher breakdown strength than BST ceramics [10, 11]. Therefore, we prepared the composite materials consisted of two phases in order to combine the excellent dielectric properties of BST with the high breakdown strength of Al_2O_3. The X-ray diffraction (XRD) confirmed the compositions. The Al_2O_3 additives improved the breakdown strength of BST ceramics, which was further discussed considering the microstructure and compositions.

D. Yi · J. Yuan · H. Liu · Y. Shen · Y.-H. Lin (✉) · C.-W. Nan
State Key Lab of New Ceramics and Fine Processing, Department of Materials Science and Engineering, Tsinghua University, Beijing 100084, People's Republic of China
e-mail: linyh@mail.tsinghua.edu.cn

X. Xi · J. He
Department of Electrical Engineering, Tsinghua University, Beijing 100084, People's Republic of China

2 Experimental procedure

The nanoscaled $Ba_{0.5}Sr_{0.5}TiO_3$ powders were prepared by the method reported by Qi et al. [12]. $Ba(NO_3)_2$, $Sr(NO_3)_2$, NaOH and $Ti(OC_4H_9)_4$ were employed as the raw materials (all reagents are analytical purity). The phase compositions and particle sizes of the as-grown $Ba_{0.5}Sr_{0.5}TiO_3$ (BST) powders were confirmed by XRD and scanning electron microscopy (SEM). The molar ratio of Al_2O_3 to BST was 0, 0.2, 0.25 and 0.5 respectively abbreviated as BST-A0, BST-A1, BST-A2 and BST-A3. The as-prepared BST powders were dispersed in ethanol by ball-grinding for a certain time. Then they were mixed homogeneously with the Al-solution, which contained certain amount of $Al(NO_3)_3$ corresponding to the different ratio above, by ultrasonic agitation. Ammonia was subsequently added until the reaction was completed. The precipitants were filtered and washed carefully for several times before they were dried and calcined at different temperatures (350–1050 °C). Then the precursor powders were pressed to green pellets (12 mm in diameter) and sintered at 1250 °C for 3 h in air.

The phase compositions of the as-prepared powders and as-sintered samples were measured by the XRD (Rigaku, D/max-RB, Cu Kα radiation). The microstructure of the as-sintered samples was studied by the SEM (Shimadzu Corporation, SSX-550). The ceramic samples for electrical measurements were polished to around 1.5 mm in thickness and pasted by silver paste on both sides, followed by 600 °C heat treatment for 20 min. The dielectric response was measured by the HP 4194A over the frequency from 100 Hz to 2 MHz. To determine the breakdown voltage, a DC load from the high voltage power source (CS 2674C, Changshen corp.) was applied to the samples immersed in silicone oil.

3 Results and discussion

Figure 1 shows the XRD patterns of the as-prepared powders calcined at 350 °C, 650 °C, 850 °C, 1050 °C and the samples sintered at 1250 °C respectively. The molar ratios are all 0.2. The XRD patterns reveal that the crystallized BST exists during the heating process. The peaks of BST move slightly to the higher angle as the temperature increases, which indicates the decrease of lattice parameter and is consistent with other studies [12, 13]. $Al(OH)_3$ is observed at low temperature and disappears as the temperature increases due to the decomposition. At 850 °C, no peaks related with Al_2O_3 are detected in the current resolution. The emergence of several extra peaks at high temperature reveals that BST reacts with Al_2O_3. At high temperature, Barium Aluminum Titanium Oxides (mainly $Ba_{1.23}Al_{2.46}Ti_{5.54}O_{16}$, labeled as BATO) and Barium Aluminum Oxides (mainly $BaAl_2O_4$, labeled as BAO) are observed. The Barium Strontium Aluminum Oxides (mainly

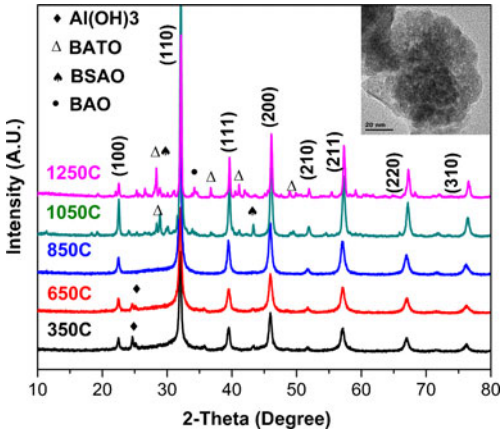

Fig. 1 XRD patterns of the as-prepared powders calcined at 350°C, 650°C, 850°C, 1050°C and the samples sintered at 1250°C respectively. The inset is the TEM photograph of the powders calcined at 350°C. The molar ratio of Al_2O_3 to BST is 0.2

$Ba_{0.6}Sr_{2.4}Al_2O_6$, labeled as BSAO) also forms to keep the chemical composition ratio. However since the XRD patterns of these oxides are complicated and overlap with each other, it is not easy to analyze them quantitatively. The inset is the TEM photograph of the powders calcined at 350 °C, and the size of the BST core is around 50 nm.

We also compare the phase compositions of the as-sintered samples with different molar ratios of Al_2O_3/BST (Fig. 2). When the ratio of Al_2O_3 to BST is low (BST-A1 and BST-A2), the phase compositions are the same as we analyze above. As the content of Al_2O_3 increases (BST-A3), Barium Aluminum Oxides (BAO) and Strontium Aluminum Oxides (SAO) are detected. Besides, there are also extra weak peaks of Al_2O_3 in the pattern of BST-A3. The changes of the phase compositions with different molar ratio can be explained as following. At high temperature, Al_2O_3 reacts with BST. BATO and BSAO form when the content of Al_2O_3 is low. As the content of Al_2O_3 increases, BATO will

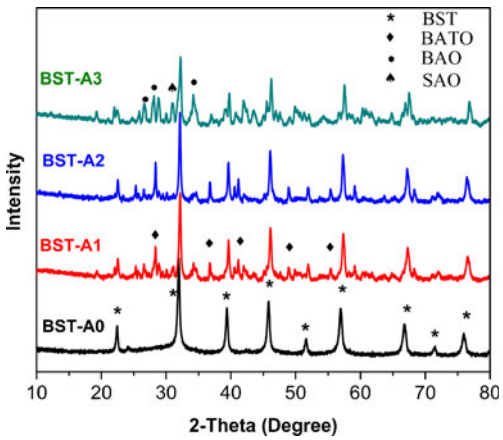

Fig. 2 XRD patterns of the as-sintered samples with different molar ratio of Al_2O_3 to BST. The ratio is 0, 0.2, 0.25 and 0.5 for BST-A0, BST-A1, BST-A2 and BST-A3 respectively

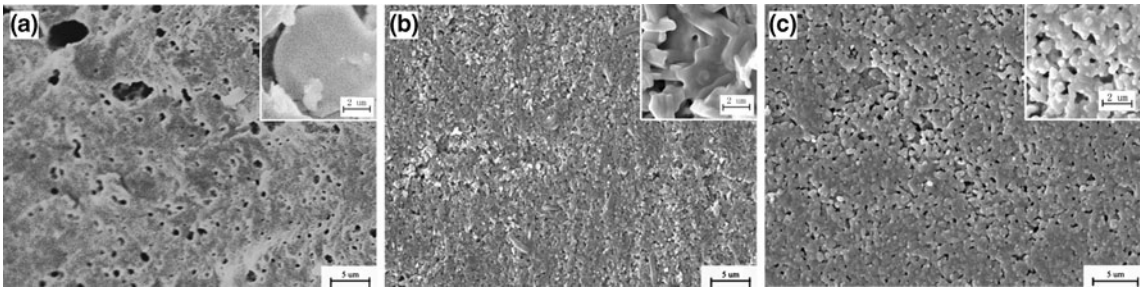

Fig. 3 SEM micrographs of the Al_2O_3-added BST ceramics: (**a**) BST-A0; (**b**) BST-A1; (**c**) BST-A2. Insets are micrographs with higher magnification

be more Al-rich, which leads to the formation of BAO/SAO. Besides, certain amount of Al_2O_3 remains unreacted due to the limited sintering time and temperature.

The microstructure of pure BST and Al_2O_3-added BST ceramics were observed by the SEM. Figure 3 shows the SEM micrographs of (a) BST-A0, (b) BST-A1 and (c) BST-A2, which reveal the relationship between Al_2O_3 additives and the grain growth as well as the microstructure developments. The grain size of Al_2O_3-added BST (~1–3 μm) is smaller than that of the pure BST, which can be seen clearly by comparing the insets in Fig. 3. Besides, the grain size decreases as the amount of Al_2O_3 increases. Similar phenomena have been reported by Q. Zhang et al. [6] in the study of BST ceramics with glass additives. In general, the size of pores in the ceramics reduces when certain amount of Al_2O_3 is added (BST-A1). In pure BST (BST-A0), the average pore size is about 2–4 um, as shown in Fig. 3(a). In BST-A1, the average pore size is about 300 nm comparing with about 1 um in BST-A2. Besides, the number of pores is less in BST-A1 based on counting in different areas. Previous works [6, 14] have reported the refinements of microstructure and the elimination of pores by using different additives in BST, which is also observed in our work. It is likely that the small amount of Al_2O_3 surrounding the BST particles act as binder to join the BST grains together during the sintering process.

Figure 4 shows the dielectric constant versus frequency for different samples. As the content of Al_2O_3 increases, the dielectric constant decreases slightly. The decline of the dielectric constant is mainly resulted from the formation of the second phases, which have relatively low dielectric constant. The reduction of Ba in BST can also lead to the decrease in dielectric constant. However, we don't see distinct shift of the BST peaks in Fig. 2 when comparing BST-A1, BST-A2 and BST-A3, which indicates that the reduction of Ba is not the main reason. X. Liang et al. have reported similar result that Al_2O_3 additives decrease the dielectric constant [15]. The dielectric constant is stable during the whole range of frequency from 100 Hz to 2 MHz for all groups except BST-A3, which indicates that over-addition of Al_2O_3 seriously destroys the dielectric properties of BST.

The breakdown strength (BDS) of the composite ceramics is also correlated with Al_2O_3 content, which is shown in Fig. 5. Pores are believed to be a very important factor to determine the breakdown strength of the ceramics since the gas discharge occurs within pores [14, 16]. Besides, several other factors, such as the grain size and the sample thickness, also change the breakdown behavior [6, 9, 17]. In addition, the intrinsic property of materials is another essential factor when considering the breakdown strength. Figure 5 shows that the samples with higher content of Al_2O_3

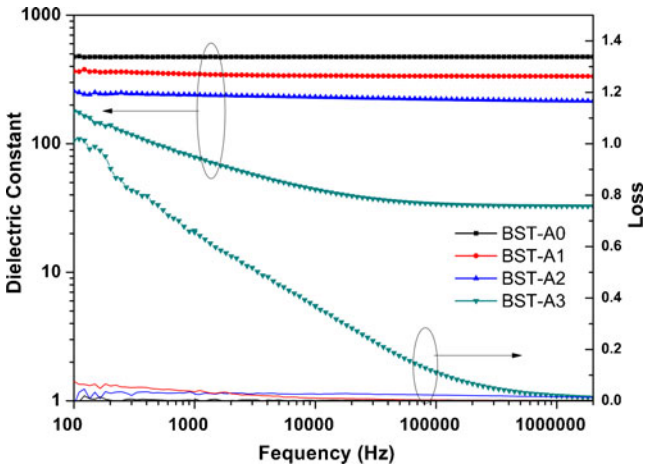

Fig. 4 Dielectric constant and loss versus frequency for BST-A0, BST-A1, BST-A2 and BST-A3 respectively

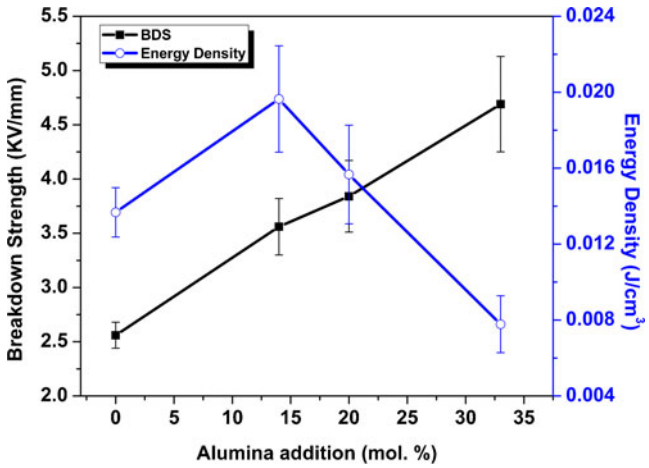

Fig. 5 Breakdown strength (BDS) and energy density of the Al_2O_3-added BST ceramics with different content of Al_2O_3

tend to show higher breakdown strength. The breakdown strength of BST-A3, which is the highest among all groups, is almost 2.1 times higher than that of the pure BST. When the content of Al_2O_3 is relatively low, the microstructure of the samples is refined. The decrease of the pore numbers and sizes is probably the main reason for the increase of breakdown strength. However, large amount of Al_2O_3 leads to more pores (Fig. 3). The further increase of breakdown strength is likely to result from the formation of the second phases, which have higher breakdown strength. In fact, these two factors act simultaneously, which lead to the great potential to increase the breakdown strength of ceramics.

The maximum energy density of the samples can be estimated by the formula:

$$U = \frac{1}{2}\varepsilon_0\varepsilon_r E^2$$

where ε_0 is the vacuum permittivity, ε_r is the relative permittivity and E is the breakdown strength. It is shown by Fig. 5 that BST-A1, with the molar ratio of Al_2O_3/BST 0.2, has the highest energy density, which is nearly 1.5 times higher than that of pure BST. The energy density is determined by both the dielectric constant and the breakdown strength. Al_2O_3 additive improves the breakdown strength and thus increases the energy density by nearly 1.5 times.

4 Conclusion

We prepared the Al_2O_3/BST two-phase composite ceramics. Our results indicate that the addition of Al_2O_3 improves the breakdown strength of BST, which can be attributed to the refinements of the microstructure and the formation of the second phases. The dielectric constant decreases slightly as the content of Al_2O_3 increases. The estimated energy density is greatly improved by the Al_2O_3 additive. The samples with the molar ratio of Al_2O_3 to BST 0.2 (BST-A1) have the highest energy density, which is about 1.5 times higher than that of pure BST. The result reveals that it is promising to increase the energy density by forming the two-phase composites and further optimization is needed for this system.

Acknowledgements This work was supported by the Ministry of Science and Technology of China through a 973-Project under Grant No. 2009CB623303, NSF of China (50737001, 50972068), NSF of Beijing 2092016 and Scientific Research Project of Tsinghua University No.2009THZ08063.

References

1. A.S. Bhalla, R. Guo, R. Roy, Mater. Res. Innov. **4**(1), 3–26 (2000)
2. W. Prellier, M.P. Singh, P. Murugavel, J. Phys. Condens. Matter **17** (30), R803–R832 (2005)
3. I. Burn, D.M. Smyth, J. Mater. Sci. **7**(3), 339–343 (1972)
4. N.H. Fletcher, A.D. Hilton, B.W. Ricketts, J. Phys. D: Appl. Phys. **29**(1), 253–258 (1996)
5. A. Young, G. Hilmas, S.C. Zhang, R.W. Schwartz, J. Am. Ceram. Soc. **90**(5), 1504–1510 (2007)
6. Q. Zhang, L. Wang, J. Luo, Q. Tang, J. Du, J. Am. Ceram. Soc. **92** (8), 1871–1873 (2009)
7. A. Herczog, IEEE Trans. Parts Hybrids Packag. **9**(4), 247–256 (1973)
8. E.P. Gorzkowski, M.J. Pan, B. Bender, C.C.M. Wu, J. Electroceram. **18**(3–4), 269–276 (2007)
9. H. Ogihara, C.A. Randall, S. Trolier-McKinstry, J. Am. Ceram. Soc. **92**(8), 1719–1724 (2009)
10. M. Touzin, D. Goeuriot, C. Guerret-Piecourt, D. Juve, H.-J. Fitting, J. Eur. Ceram. Soc. **30**(4), 805–817 (2010)
11. H. Bartzsch, D. Glob, P. Frach, M. Gittner, E. Schultheib, W. Brode, J. Hartung, Phys. Status Solidi A **206**(3), 514–519 (2009)
12. J.Q. Qi, Y. Wang, W.P. Chen, L.T. Li, H.L.W. Chan, J. Solid State Chem. **178**(1), 279–284 (2005)
13. H.Y. Tian, J.Q. Qi, Y. Wang, H.L.W. Chan, C.L. Choy, Nanotechnology **16**(1), 47–52 (2005)
14. G. Dong, S. Ma, J. Du, J. Cui, Ceram. Int. **35**(5), 2069–2075 (2009)
15. X. Liang, W. Wu, Z. Meng, Mat. Sci. Eng.: B **99**(1–3), 366–369 (2003)
16. P. Duran, F. Capel, J. Tartaj, C. Moure, J. Am. Ceram. Soc. **84**(8), 1661–1668 (2001)
17. T. Tunkasiri, G. Rujijanagul, J. Mater. Sci. Lett. **15**(20), 1767–1769 (1996)